TISSUE ENGINEERING: Part A
Volume 20, Numbers 19 and 20, 2014

DOI: 10.1089/ten.tea.2013.0583

Fabrication and *In Vivo* Microanastomosis of Vascularized Tissue-Engineered Constructs

Rachel Campbell Hooper, MD, Karina A. Hernandez, DO, Tatiana Boyko, MD, Alice Harper, BA, Jeremiah Joyce, BA, Alyssa R. Golas, MD, and Jason A. Spector, MD

Tissue engineering endeavors to create replacement tissues and restore function that may be lost through infection, trauma, and cancer. However, wide clinical application of engineered scaffolds has yet to come to fruition due to inadequate vascularization. Here, we fabricate hydrogel constructs using Pluronic® F127 as a sacrificial microfiber, creating microchannels within biocompatible, biodegradable type I collagen matrices. Microchannels were seeded with human umbilical vein endothelial cells (HUVEC) or HUVEC and human aortic smooth muscle cells (HASMC) in co-culture, generating constructs with an internal endothelialized microchannel. Histological analysis demonstrated HASMC/HUVEC-seeded constructs with a confluent lining after 7 days with preservation and further maturation of the lining after 14 days. Immunohistochemical staining demonstrated von Willebrand factor and $CD31^+$ endothelial cells along the luminal surface (neointima) and alpha-smooth muscle actin expressing smooth muscle cells in the subendothelial plane (neomedia). Additionally, the deposition of extracellular matrix (ECM) components, heparan sulfate and basal lamina collagen IV were detected after 14 days of culture. HUVEC-only- and HASMC/HUVEC-seeded microchannel-containing constructs were microsurgically anastomosed to rat femoral artery and vein and perfused, *in vivo*. Both HUVEC only and HUVEC/HAMSC-seeded constructs withstood physiologic perfusion pressures while their channels maintained their internal infrastructure. In conclusion, we have synthesized and performed microvascular anastomosis of tissue-engineered hydrogel constructs. This represents a significant advancement toward the generation of vascularized tissues and brings us closer to the fabrication of more complex tissues and solid organs for clinical application.

Introduction

Microsurgical free tissue transfer has transformed the field of reconstructive surgery. This technique affords surgeons the ability to transplant composite tissues (i.e., skin and muscle, skin and fascia) known as flaps, with an accompanying blood supply to and from anywhere in the body.[1,2] As opposed to traditional grafting, which relies upon neoangiogenesis from the recipient wound bed to reestablish perfusion within the transferred tissue, large volumes of autologous tissue can be reliably transferred via the immediate reestablishment of tissue perfusion by microsurgical anastomosis to the patient's recipient vasculature. Although it has become routine, current clinical application may be limited by the availability of suitable donor tissue or marred by the obligatory donor-site morbidity including pain, scarring, functional loss, and poor wound healing that can result following tissue harvest.[1,2]

A number of complex tissues and solid organs have been engineered for reconstruction and/or restoration, including skin, trachea, ears, liver, kidney, heart, and lungs.[3–9] With the exception of cartilage, which is devoid of intrinsic vascularity, all other tissues require an inherent vascular network for survival. As such, virtually any clinical application of human scale-engineered tissues requires a design with an integrated and hierarchical vascular network that may be anastomosed to the host vasculature to preserve the viability of the cellular constituents. Currently, there are a number of clinically available acellular and cell-based tissue-engineered products,[8,9] which are all applied as grafts, thereby significantly limiting their clinical application to optimal wound beds. Specifically, with grafts vascular ingrowth and incorporation are inconsistent and require extended periods of time (weeks),[9,10] predisposing patients to several complications including infection, venous thromboembolism, and potentially graft loss.

The fabrication of tissues that replicates the complex hierarchal micro and macrovascular organization found *in vivo* continues to pose a major obstacle. For example,

Laboratory for Bioregenerative Medicine and Surgery, Division of Plastic Surgery, Weill Cornell Medical College, New York, New York.

the spontaneous formation of capillaries within a tissue-engineered construct via the culture of fibroblasts and endothelial cells with or without keratinocytes has been described; however, these also rely on host ingrowth for incorporation and ultimate survival, limiting their applicability.[11,12] While significant progress has been made toward understanding neovascularization, angiogenesis, and vasculogenesis in an effort to generate vascularized tissue-engineered constructs,[13–18] we have yet to see the creation of vascular networks that faithfully recapitulates the organization that exists *in vivo*. Furthermore, there has been no published report of a *de novo* tissue-engineered construct with a vascular channel/network that may be surgically connected to the host.

A number of polymers including sucrose,[19] carbohydrate glass[20] (a combination of glucose, sucrose, and dextran), shellac,[21] and alginate[22] have been utilized as sacrificial microfibers to create vascular networks within a bulk polymer. In previous work, we employed a sacrificial microfiber technique whereby three-dimensional (3D) vascular networks were cast within a polydimethylsiloxane (PDMS) bulk using sacrificial melt-spun sucrose with 1 mm sucrose inlet and outlet sticks, forming the hierarchal architecture of a capillary bed, feeding artery, and draining vein respectively.[19] This intrinsic vascular network supported perfusion of erythrocytes with pressure gradients within physiologic parameters. However, as these constructs were fabricated from PDMS, cell seeding and biodegradation was not possible. To address this significant limitation we have modified the compositions of our bulk and sacrificial materials, using collagen and Pluronic® F127 respectively, resulting in tissue-engineered constructs capable of supporting cell engraftment, microsurgical anastomosis, and *in vivo* perfusion.

Materials and Methods

Collagen extraction/neutralization

Tendons excised from rat tails (Pel-Freez® Biologicals, Rogers, AK) were suspended in 0.1% acetic acid 75 mL/g of tendon. After 72 h at 4°C, the collagen solution was centrifuged for 90 min at 8800/*g*. The supernatant solution was collected, frozen, and lyophilized. A stock solution of collagen (15 mg/mL) was prepared by dissolving lyophilized collagen in 0.1% acetic acid and neutralized on ice using Medium 199 (Gibco®, Life technologies, Grand Island, NY) and NaOH until pH 7.4 was reached.

Sacrificial microfiber fabrication

A PDMS mold with 1 mm longitudinal pattern and 1.5 mm loop pattern was created (Fig. 1a). Pluronic F127 (Sigma-Aldrich®, St. Louis, MO) was heated to 65°C and placed into PAM® (Congra Foods, Omaha, NE) coated, prepatterned PDMS molds. Microfibers were allowed to solidify at −20°C for 5 min and demolded (Fig. 1b). Fabricated microfibers were stored at room temperature until ready for use.

Scaffold fabrication and cell seeding

$15 \times 15 \times 5$ mm reservoirs were created within a PDMS mold, in which 14- or 16-gauge catheters were placed, forming an inlet and outlet in the central mold (Fig. 1c, d). For *in vivo* microanastomosis, two holes were cut into a piece of polyglactone mesh (Ethicon®, Bridgewater, NJ) and carefully aligned with the construct inlet and outlet to provide a means of suture fixation. Neutralized collagen was manually extruded over the microfibers and the constructs underwent thermal gelation at 37°C for 30 min. Human umbilical vein endothelial cells (HUVEC) were cultured in Media 199 1× supplemented with endothelial mitogen (EM©; Biomedical Technologies, Inc., Stoughton, MA), heparin sodium salt (Sigma-Aldrich, St. Louis, MO), fetal bovine serum (FBS, Hyclone©; Thermo Scientific, Logan, UT), glutamine (Glutamax-100×; Gibco, Life Technologies), HEPES 1 M buffer (Lonza©, Walkersville, MD), and penicillin/streptomycin. Human aortic smooth muscle cells (HASMC) were cultured in Media 199 supplemented with FBS, EM, heparin, and penicillin/streptomycin. Media was changed every other day for both cell lines. On the day of seeding, cells were trypsinized and counted using a standard hemocytometer. Sixty microliters of a 5×10^6 cells/mL solution was injected into the inlet of the loop and longitudinal microchannels respectively. For co-culture studies, HASMC were split, counted, and seeded as above, with HUVEC seeded after 24 h. All scaffolds were cultured under static conditions for 7 and 14 days with daily media changes.

Scaffold implantation

Nude rats (NU/NU 316; Charles River, Kingston, NY) were used for this study. All animals were provided with chow and water *ad libitum* and maintained in a climate control facility accredited by the Association for Assessment and Accreditation of Laboratory Animal Care. All

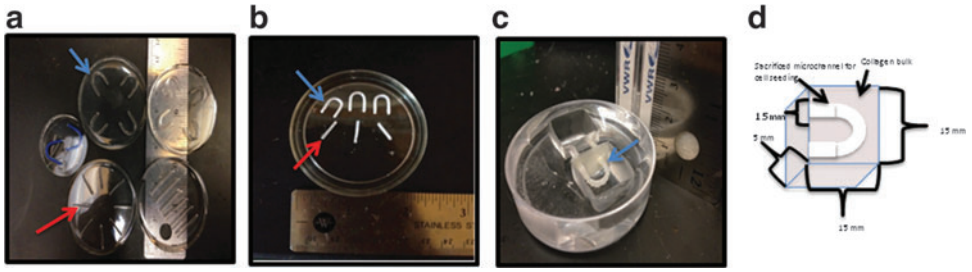

FIG. 1. Sacrificial microfiber fabrication. **(a)** Polydimethylsiloxane (PDMS) molds for fabrication of Pluronic® F127 loop (blue arrow) and longitudinal (red arrow) microfibers. **(b)** Microfibers following solidification and demolding. **(c)** Sacrificial Pluronic F127 longitudinal microchannel within reservoir prior to hydrogel embedding. **(d)** Sacrificial loop microchannel prior to hydrogel embedding. Color images available online at www.liebertpub.com/tea

animal experiments were in compliance with the Guide for the Care and Use of Laboratory Animals[30] and the Weill Cornell Medical College Institutional Animal Care and Use Committee approved this protocol (2011-0086). Rats were weighed and anesthetized via intraperitoneal (IP) injection of ketamine (80–90 mg/kg) and xylazine (4–8 mg/kg). A member of the research team manually monitored heart rate and respirations during the entire procedure. One 6 cm linear incision was made in the infrainguinal region, with dissection carried through the subcutaneous tissues down to the femoral vessels with ligation of any branches. The femoral artery and vein were skeletonized and clamped proximally and ligated distally. The vessels were flushed with heparinized saline and dilated. Just prior to the start of microsurgical anastomosis, 80 U/kg heparin (Heparin Sodium; Sagent Pharmaceuticals©, Schaumburg, IL) was administered IP. With the aide of an operating microscope, an end-to-end anastomosis with interrupted 9-0 nylon microsuture (Sharpoint™; Surgical Specialties Corp, Reading, PA) was performed between the femoral artery and vein and polyglactone mesh of construct inlet and outlet respectively. Microdoppler assessment and venous strip tests where the vein is ''stripped'' or emptied, occluded proximally and distally, and then released proximally, were used to demonstrate anterograde flow. A total of 14 constructs were implanted, 2 unseeded, 7 HUVEC-only-seeded cultured for 7 days prior to implantation, and 5 HUVEC/HASMC-seeded constructs cultured for 14 days prior to implantation.

Multiphoton microscopy

Entire constructs were imaged using an Olympus FluoView FV1000MPE multiphoton microscope (Olympus America, Center Valley, PA). Prior to imaging, scaffolds were fixed in 10% buffered formalin. All specimens were imaged using a 10X/0.60NA water immersion objective. A femtosecond pulsed titanium/sapphire laser (Mai Tai HP, Spectra-Physics; Newport Corporation, Irvine, CA) at 780 nm was used to excite the specimens. Optical sections were acquired in 10 μm slices for stacks up to 400 μm. Short wavelength autofluorescent (420–490 nm, color coded green) intrinsic tissue emission signals were collected, originating in part from reduced nicotinamide adenine dinucleotide and flavin adenine dinucleotide in the cytoplasm of cells. Post-processing of .stk files was completed using Image J software (NIH, Bethesda, MD).

Functional studies

Functionality of seeded endothelial cells within scaffold microchannels was assessed via receptor-mediated endocytosis of acetylated low density lipoprotein (Invitrogen®, Eugene, OR). A 10 μg/mL suspension was injected into the inlet of seeded microchannels and allowed to incubate for 16 h. Following incubation, scaffolds were fixed and imaged *in situ* via fluorescent microscopy (Olympus IX71; Olympus America).

Histology and immunohistochemistry

Scaffolds were fixed in 10% buffered formalin and underwent vacuum tissue infiltration processing, paraffin embedding, and microtome sectioning. Hematoxylin and eosin (H&E) staining was performed on 10 μm sections of each scaffold. Stained sections were imaged with bright field microscopy (Olympus IX71; Olympus America) to determine cellularity. Immunohistochemical staining was performed using rabbit polyclonal anti-CD31/platelet endothelial cell adhesion molecule (Abcam© Cambridge, MA), rabbit polyclonal anti-von Willebrand factor (vWF; Abcam©), mouse monoclonal anti-collagen IV, mouse monoclonal anti-alpha-smooth muscle actin (α-SMA; Invitrogen), and counterstained with 4′,6-diamidino-2-phenylindole (DAPI; Invitrogen). Standard deparaffinization, rehydration, and antigen retrieval steps were performed per manufacturer's recommendations. Specimens were incubated with primary antibody for 16 h at 4°C and secondary antibodies for 1 h at room temperature. After secondary antibody staining, specimens were mounted and imaged via fluorescent microscopy (Olympus IX71; Olympus America). To determine the composition of elaborated matrix proteins within co-cultured microchannels, 10 μm sections were stained with FITC-*Lycopersicon esculentum* (Sigma-Aldrich, St. Louis, MO) to identify the heparan sulfate.

Results

Scaffold fabrication and cell seeding for in vitro *studies*

Our design for Pluronic® F127 loop (Fig. 1e) and longitudinal microfibers reliably formed microchannels within our collagen hydrogels and *in vitro* patency was confirmed via media perfusion through the inlet with passage via the outlet prior to cell seeding. HASMC were seeded 24 h prior to HUVEC seeding to reconstitute proper anatomic configuration and establish mural support and elaboration of growth and binding factors, promoting HUVEC attachment, proliferation, and stability. All constructs were cultured under static conditions for 7 and 14 days.

Multiphoton microscopy demonstrated HUVEC only-seeded microchannel containing constructs with adherent endothelial cells along the luminal surface (Fig. 2a, b and Supplementary Video S1; Supplementary Data are available online at www.liebertpub.com/tea). HASMC/HUVEC-seeded microchannel-containing collagen constructs had a heterogeneous confluent cellular layer lining the surface of the microchannel (Fig. 2c, d and Supplementary Video S2). Histological analysis confirmed cellular adhesion with spontaneous organization into a concentric layered pattern within HAMSC/HUVEC-seeded microchannels after 7 days (Fig. 2e, f). In contrast, HUVEC-only-seeded microchannels demonstrated areas of cell delamination with no deposition of extracellular matrix (ECM) after 7 days of culture (Fig. 2g, h). Following 14 days, HUVEC/HASMC-seeded microchannels demonstrated proliferation of smooth muscle cells within the ''neomedia'' (Fig. 3a, b) with ''neointimal'' endothelial cells maintained along the luminal surface. Moreover, cells began to remodel the original collagen matrix, migrating laterally from the microchannel into the bulk, forming angiogenic ''sprouts'' (Fig. 3c) with CD31 expressing endothelial cells (Fig. 3d). However, after 14 days HUVEC only-seeded microchannels exhibited areas of cellular detachment without additional matrix protein synthesis, remodeling, or cell migration (data not shown).

To specifically characterize the type and spatial distribution of the seeded cells along the microchannel immunohistochemical staining was performed. After 7 days, $CD31^+$ and

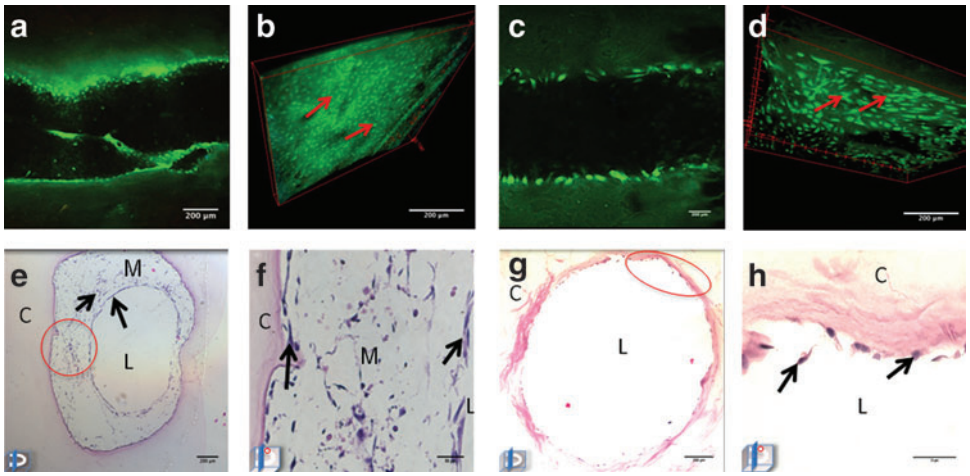

FIG. 2. Multiphoton microscopy and hematoxylin and eosin (H&E) staining of human umbilical vein endothelial cells (HUVEC) and HUVEC/human aortic smooth muscle cells (HASMC)-seeded microchannels after 7 days of static culture. Coronal multiphoton micrograph after 7 days of culture in a microchannel seeded with HUVEC **(a)** and three-dimensional (3D) reconstruction **(b)** of optical stack with adherent autoflourescent cells along microchannel luminal wall. **(c)** Coronal multiphoton micrograph of HUVEC/HASMC-seeded microchannel and 3D reconstruction **(d)** after 7 days of culture depicting a confluent lining of cells along the luminal surface. H&E-stained HASMC/HUVEC-seeded microchannel **(e, f)** and HUVEC-only-seeded microchannel **(g, h)** after 7 days. Note the areas of HUVEC delamination within HUVEC-only-seeded microchannels (oval). Color images available online at www.liebertpub.com/tea

vWF expressing endothelial cells were identified along the luminal surface (Fig. 4a, b), with α-SMA expressing smooth muscle cells in the subendothelial plane. This spatial relationship was largely preserved after 14 days with $CD31^+$ and vWF expressing endothelial cells along the luminal surface and additional layers of α-SMA expressing smooth muscle cells comprising the neomedia (Fig. 4c, d). Furthermore, after 14 days, deposition of heparan sulfate (Fig. 4e, f) and basal lamina protein collagen IV (Fig. 4g–i) was detected along the abluminal surface of $CD31^+$ endothelial cells. Functionality of the neointima was confirmed via acetylated low-density lipoprotein receptor-mediated endocytosis in both HUVEC-only- and HASMC/HUVEC-seeded microchannels after 7 and 14 days (Fig. 4j–m).

In vivo *implantation studies*

The ''loop'' configuration, modified with polyglactin mesh (Fig. 5a) proved more suitable for *in vivo* anastomosis as it placed the least amount of tension on the vessels and more closely recapitulates the native anatomy of the adjacent artery and vein (Fig. 5b, c). Constructs were successfully

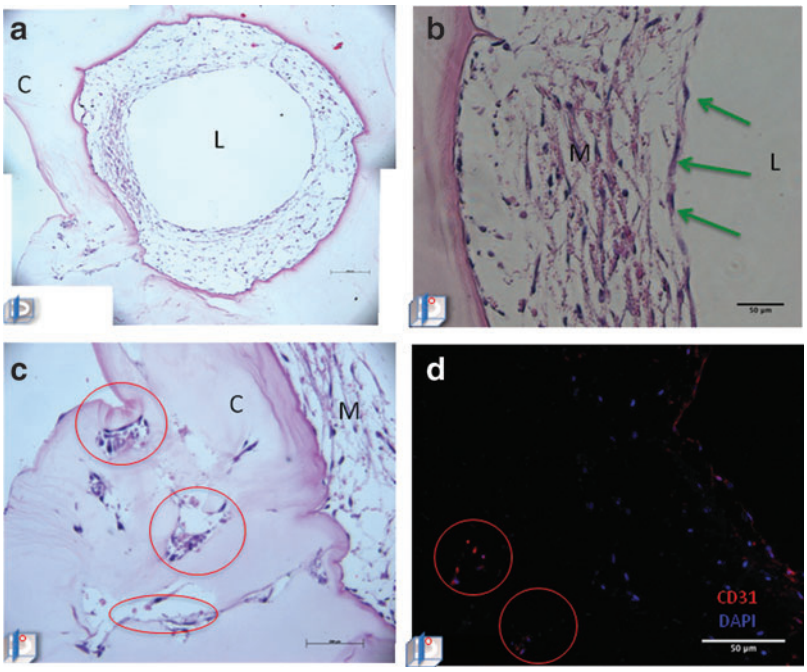

FIG. 3. Angiogenic sprouts, neomedial and neointimal layers formed within HUVEC/HASMC-seeded microchannels after 14 days. **(a)** HUVEC/HASMC-seeded microchannel after 14 days of culture with **(b)** higher magnification demonstrating neointimal and neomedial layers. **(c)** Areas of lateral invasion and the formation of **(d)** angiogenic sprouts (encircled) confirmed via CD31 expression. (C, construct; L, lumen; M, matrix proteins; image in left lower corner represents the plane of section through the microchannel.) Color images available online at www.liebertpub.com/tea

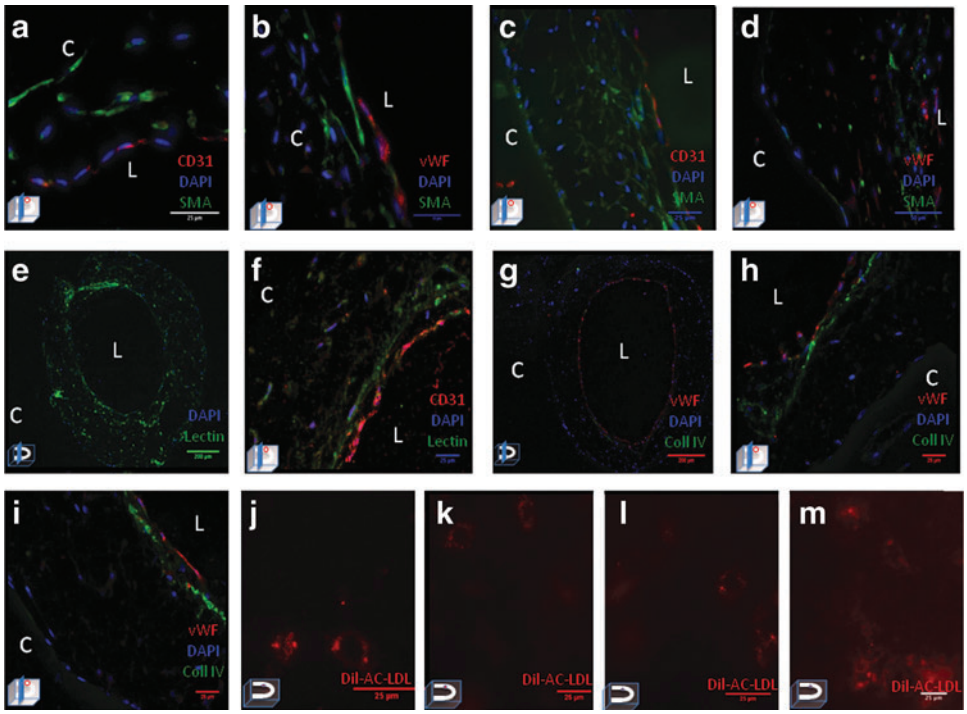

FIG. 4. Immunohistochemical staining of HUVEC and HASMC/HUVEC-seeded microchannels after 7 and 14 days. HUVEC/HASMC-seeded microchannels stained for CD31, von Willebrand factor (vWF), and alpha-smooth muscle actin (α-SMA) after **(a, b)** 7 and **(c, d)** 14 days. Note $CD31^+$ and vWF expressing HUVEC along the luminal (L) surface and α-SMA expressing SMC in the subendothelial plane. *Lycopersicon esculentum* stained microchannel after **(e)** 14 days demonstrating heparan sulfate within the neointimal glycocalyx and neomedia extracellular matrix (ECM), co-localized with $CD31^+$ **(f)**. **(g)** HASMC/HUVEC-seeded microchannel with vWF^+ endothelial cells along the luminal surface and basal lamina Collagen IV (green) in the abluminal plane. **(h, i)** Co-localized vWF^+ (red) endothelial cells with basal lamina collagen IV. *In situ* fluorescent imaging of **(j)** HUVEC-only-seeded microchannel and **(k)** HUVEC/HASMC-seeded microchannel after 7 days of static culture depicting acetylated low density lipoprotein uptake demonstrating endothelial cell functionality. **(l)** HUVEC-only- and **(m)** HAMSC/HUVEC-seeded microchannels depicting acetylated low density lipoprotein uptake and endothelial cell functionality within the microchannel following 14 days of culture. (Image in left lower corner represents the plane of section through the microchannel.) Color images available online at www.liebertpub.com/tea

anastomosed to *Nu/Nu* 316 rats (Fig. 5d). Upon unclamping the recipient vein, the internal microchannel was filled with dark deoxygenated venous blood (Fig. 5e). Following unclamping of the inflow femoral artery, the microchannel was immediately perfused with bright red oxygenated blood (Fig. 5f).

Patency and anterograde flow was confirmed via microdoppler auscultation of pulsatile blood flow along the microchannel (Supplementary Video S3) within the construct. Venous strip resulted in prompt filling of the previously empty segment, indicative of anterograde flow (Supplementary Video S4). Rat femoral mean arterial pressures are 81–100 mmHg,[23–25] and our constructs withstood physiologic perfusion pressure with maintenance of the microchannel infrastructure. Following completion of microanastomosis, animals were allowed to emerge from anesthesia and resumed normal activity. Fourteen constructs were implanted. Initially, two unseeded constructs were implanted, then seven HUVEC-only-seeded constructs cultured under static conditions for 7 days prior to implantation were implanted. Given our *in vitro* results and the appearance of the endothelial lining, we transitioned to HASMC/HUVEC-seeded constructs and implanted a total of five additional constructs that were cultured under static conditions for 14 days prior to implantation. The duration of implantation *in vivo* ranged from 15 min to 24 h. *In vivo* experiments were terminated at the time of thrombosis or if the animals expired secondary to bleeding or anesthesia. Thrombosis occurred ~50% of the time, although it is unclear if the thrombosis occurred at the site of anastomosis or within the construct itself. In all cases, constructs were retrieved, fixed, and processed for histology.

Postperfusion H&E analysis of unseeded microchannels demonstrated adhesion of polymorphonuclear leukocytes along the luminal surface in a time-dependent manner (Fig. 5g–j), whereas in HUVEC-only seeded constructs a confluent layer of $CD31^+$ endothelial cells was maintained along the microchannel lumen (Fig. 5k, l). Furthermore, in contrast to unseeded microchannels, few inflammatory cells were seen along the microchannel lumen (Fig. 5m, n). Postperfusion analysis of HASMC/HUVEC seeded microchannels demonstrated a thickened and more mature HASMC/HUVEC lining that withstood physiological pressures (Fig. 5o, p). Immunohistological analysis (Fig. 5q, r) characterized this concentric carpet of cells along the luminal surface as α-SMA expressing HAMSC forming a neomedial layer, and vWF expressing HUVEC forming the neointimal layer with adjacent

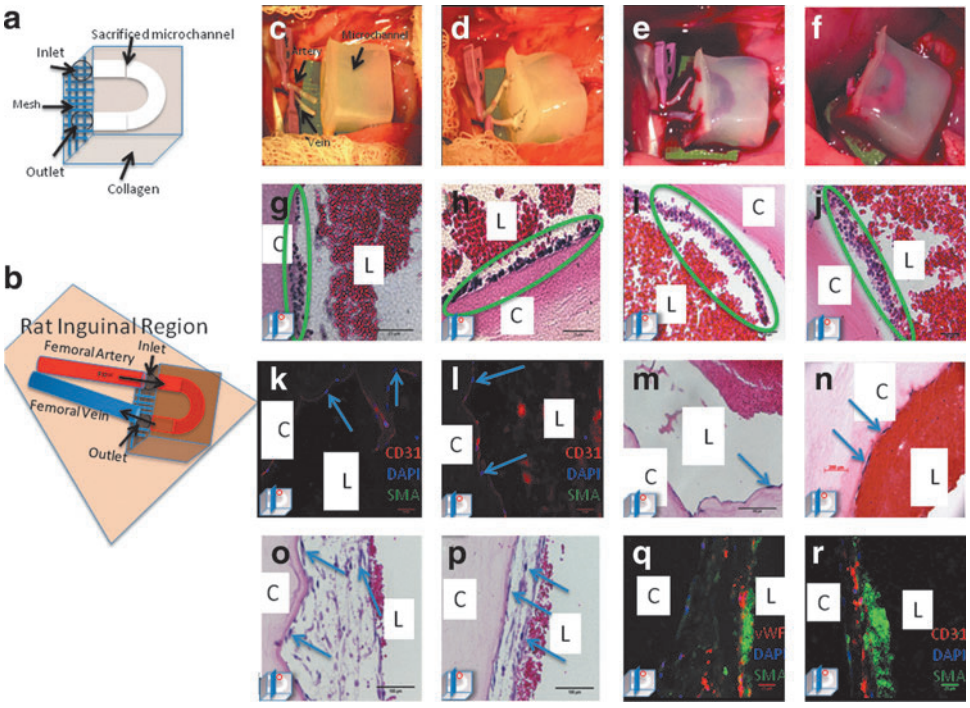

FIG. 5. *In vivo* anastomosis and perfusion of endothelialized microchannel-containing constructs. **(a)** Design of constructs for implantation with the addition of polyglactone mesh. **(b)** Schematic of anastomotic sites. Construct *in situ* just prior to anastomosis with femoral vessels dissected and clamped **(c)**, upon completion of microanastomosis **(d)**, with venous effluent following unclamping of outflow vessel, **(e)** and with continuous perfusion following arterial unclamping **(f)**. H&E-stained sections of unseeded constructs following *in vivo* perfusion for 2.5 **(g, h)** and 5 h **(i, j)** with accumulation of host inflammatory cells along the microchannel wall. Postperfusion analysis of seeded constructs demonstrate maintenance of HUVEC lining with $CD31^+$ **(k, l)** expressing endothelial cells along the microchannel lumen and H&E confirming no accumulation of inflammatory cells **(m, n)**. Representative H&E-stained sections of co-culture seeded constructs postperfusion **(o, p)** demonstrating a mature, thickened lining with adjacent erythrocytes. Immunohistochemical staining of co-cultured seeded constructs **(q, r)** postperfusion with vWF (red) expressing endothelial cells along the luminal surface forming the neointima and α-SMA (green) expressing HASMC in the subendothelial plane forming the neomedia; note luminal autofluroescent erythrocytes postperfusion. (Image in left lower corner represents the plane of section through the microchannel.) Color images available online at www.liebertpub.com/tea

luminal autofluorescent erythrocytes. (C, construct; L, lumen, image in left lower corner represents the plane of section through the microchannel.)

Discussion

The fabrication of thick tissues that closely replicates the complex hierarchal micro- and macrovascular environment found *in vivo* continues to pose a major obstacle. Current tissue-engineered scaffolds are typically restricted in thickness to a few millimeters, with scaffolds containing living cells being obligatorily thin, reflecting the limitations of diffusion. One of the most commonly used acellular dermal replacement matrices, Integra®, is composed of a bilayer bovine collagen-shark chondroitin-6-sulphate glycosaminoglycan matrix with silicone membrane; it is avascular and relies on host cellular invasion and neovascularization that can take up 3 weeks, during which time patients are at risk for infection and graft loss.[8–10] A number of allogenic and autologous skin substitutes are also available for clinical use including Transcyte® (synthesized from nylon mesh and neonatal foreskin fibroblasts), Dermagraft® (synthesized from polyglycolic acid mesh with neonatal foreskin fibroblasts), and selective epidermal autografts (combines autologous keratinocytes and irradiated mouse fibroblasts).[8,9] However, these are avascular and must be applied clinically as grafts thus limiting their use and presenting the same challenges as acellular matrices in terms of duration required for neovascularization and incorporation.

One popular strategy to create vascularized tissue-engineered constructs utilizes decellularization, which removes all antigenic cellular material from the target tissue while largely preserving the ECM and vascular network, leaving a scaffold that can be reseeded with vascular- and tissue-specific cells.[4–6] Schultheiss *et al.* repopulated decellularized jejunal segments with endothelial, smooth muscle, and urothelial cells to create a ''prevascularized'' bladder-like tissue; both recellularized and unrecellularized segments were surgically anastomosed to host vessels, with a maximum thrombosis-free perfusion interval of 3 h using a seeded segment.[4] Successful decellularization and recellularization of an intact liver ECM with hepatocytes has also been described.[5] Additionally, Song *et al.* produced engineered rat kidneys via decellularization and repopulation with HUVEC and rat neonatal kidney cells.[6] Although regenerated kidneys produced ''rudimentary'' urine *in vitro*,

after orthotopic transplantation the duration of perfusion was not disclosed, indicating the difficulty involved with sustainable perfusion of tissue-engineered constructs, attributable to imperfect re-endothelialization, exposure of subendothelial collagen, and likely subsequent thrombosis.

Our approach to the development of thick bioengineered tissues for clinical use relies on sacrificial polymers cast into a biocompatible matrix. We first reported this approach[19] utilizing sucrose and silicone as the sacrificial and bulk materials, respectively, generating perfusable microchannels. However, we have since transitioned to more biocompatible components to facilitate cell seeding and construct implantation. Although other groups have since reported fabrication of microvascular networks[14–17,20] within a bulk polymer, we describe successful *in vivo* anastomosis and perfusion of a *de novo* microvascular network. Special consideration was given to scaffold material chemistry so as to encourage cellular survival and subsequent scaffold integration within the host. Pluronic® F127, our sacrificial microfiber, consists of a tri-block copolymer containing a central hydrophobic core of polypropylene glycol flanked by hydrophilic polyethylene glycol. It is an FDA-approved material and is commonly found in cosmetics, mouthwashes, and contact lens solution, and here it is used to form microchannels within our matrix.[25] Type I collagen is an ideal bulk material as it is an integral component of the natural ECM, has low antigenicity, is biodegradable, biocompatible, and facilitates cellular adhesion and growth.[18]

Mural smooth muscle cells are vitally important to the formation of any microvascular lining, and assist endothelial cells via complex interactions and biochemical crosstalk with the synthesis and elaboration of growth factors, junctional molecules, and adhesion proteins.[18,26–28] As demonstrated in our study (and others), mural cells provide physical support to the endothelium promoting maturation, quiescence, and the formation of a stable confluent, functional lining.[14,26,27] Shepard *et al.* have previously demonstrated that implanted collagen scaffolds cocultured with endothelial and smooth muscle cells resulted in stable vessels without angioregresion.[29] Following 14 days of culture, we detected the elaboration of basal lamina collagen IV and the presence of heparan sulfate, a major component of the glycocalyx and the ECM that are both of critical importance to the maintenance of the endothelial lining. Additional studies have confirmed the significance of mural cells in stimulating basement membrane assembly that contributes to the stability of the endothelial lining.[14,17,21,26–29] Without smooth muscle cell support, endothelial cells are susceptible to detachment and apoptosis, a finding that is confirmed in our HUVEC-only-seeded microchannels. vWF and CD31 expression are two of the most widely cited markers of endothelial cell function *in vitro*[28]; both were widely expressed within the neointima of our seeded microchannels. Additionally, HUVEC demonstrated acetylated low density lipoprotein receptor-mediated endocytosis, indicative of a functional, active endothelial lining.

With successful endothelialization *in vitro* we next sought to evaluate our constructs *in vivo.* Prior attempts to anastomose native vessels to our hydrogel constructs were limited by the poor tensile strength of the collagen hydrogel. To overcome this obstacle, a hybrid hydrogel mesh construct was fabricated in which construct inlet and outlet zones were reinforced with polyglactone mesh. The ''loop'' configuration proved more suitable for anastomosis as it placed the least amount of tension on the vessels following microanastomosis and more closely recapitulates natural anatomy with adjacent artery and vein. Following arterial unclamping, constructs withstood physiologic perfusion pressure and maintained their microchannel infrastructure. With direct anastomosis of these tissue-engineered constructs to host vessels, the seeded and ingrowing cells are provided with immediate supply of oxygen and nutrients ensuring scaffold survival and integration. Such constructs are scalable and with internal microvasculature and immediate perfusion, there is theoretically no limit to the size and thickness of the constructs one can create.

Although completely intact constructs withstood physiologic perfusion pressure with maintenance of the microchannel infrastructure, undetectable microscopic defects (e.g., tiny bubbles or microfractures) within the hydrogel resulted in areas of weakness and potential dissection. When this occurred in our constructs, we observed areas of thrombus formation over exposed areas of collagen

This study identifies the fundamental components necessary for the fabrication of clinically relevant, vascularized tissue-engineered scaffolds that are readily scalable. We have demonstrated that a collagen matrix, with an inherent vascular framework seeded with endothelial and smooth muscle cells results in the formation of a patent, vascularized construct that can be microsurgically anastomosed and immediately perfused *in vivo*. Our approach represents a significant advancement in the field of tissue-engineering and serves as a powerful method for the fabrication of surgically-relevant replacement tissues, as this technique allows for immediate vascularization and thus survival of cellular constituents within the construct. In stark contrast to current approaches that rely upon scaffold engraftment via the host wound bed, by directly anastomosing these tissue-engineered constructs to host vessels in a manner similar to free tissue transfer, the seeded and ingrowing cells are provided with immediate supply of oxygen and nutrients ensuring scaffold survival and integration. Because of their internal microvasculature and immediate perfusion, such constructs are scalable to clinically relevant sizes, potentially eliminating the need to harvest autologous tissue for reconstruction. Furthermore, beyond their application for the fabrication of tissue replacements, these same strategies may be used to create custom-designed 3D perfusable constructs to serve as a platform for the study of any combination of cells and therapeutic molecules, *in vivo* or *ex vivo*. Lastly, while our *in vivo* results demonstrate a foreseeable transition to the clinical application of vascularized tissue-engineered constructs additional long-term perfusion studies are still necessary in the future.

Acknowledgments

The authors would like to thank Dr. Abraham Stroock and the members of his laboratory, Mrs. Leona Cohen-Could, Mr. Amit Aggarwal, and the members of the Weill Cornell Microscopy Core, Dr. Clay Bracken and Teresa and Joseph Wood. This work was supported in part by the Empire

Clinical Research Investigator Program and the Plastic Surgery Foundation (Grant # 274640).

Disclosure Statement

The authors have no competing financial interests.

References

1. Jones, N.F., Jarrahy, R., Song, J.L., Kaufman, M.R., and Markowitz, B. Postoperative medical complications—not microsurgical complications negatively influence morbidity, mortality, and true cost after microsurgical reconstruction for head and neck cancers. Plast Reconstr Surg **119,** 2053, 2007.
2. Agostini, T., Lazzeri, D., and Spinelli, G. Anterolateral thigh flap: systematic literature review of specific donor-site complications and their management. J Craniomaxillofac Surg **41,** 5, 2012.
3. Nemeno-Guanzon, J.G., Lee, S., Berg, J.R., Jo, Y.H., Yeo, J.E., Nam, B.M., Koh, Y.G., and Lee, J.I. Trends in tissue engineering for blood vessels. J BiomedBiotechnol **2012,** 956345, 2012.
4. Schultheiss, D., Gabouev, A.I., Sebotari, S., Tudorache, I., Walles, T., Schlote, N., Wefer, J., Kaufman, P.M., Haverich, A., Stief, C.G., Jonas, U., and Mertsching, H. Biological vascularized matrix for bladder tissue engineering: matrix preparation, reseeding technique and short-term implantation in a porcine model. J Urol **173,** 276, 2005.
5. Ott, H.C., Matthiesen, T.S., Goh, S.K., Black, L.D., Kren, S.M., Netoff, T.I., and Taylor, D.A. Perfusion decellularized matrix: using nature's platform to engineer a bioartificial heart. Nat Med **14,** 213, 2008.
6. Song, J.J., Guyette J.P., Glippin, S.E., Gonzalez, G., Vacanti, J.P., and Ott, H.C. Regeneration and experimental orthotopic transplantation of a bioengineered kidney. Nat Med **19,** 646, 2013.
7. Reiffel, A.J., Kafka, C., Hernandez, K.A., Popa, S., Perez, J.L., Zhou, S., Pramanik, S., Brown, B.N., Ryu, W.S., Bonassar, L.J., and Spector, J.A. High fidelity tissue engineering of patient specific auricles for reconstruction of pediatric microtia and other auricular deformities. PLoS One **8,** 1, 2013.
8. Alrubaiy, L., and Al-Rubaiy, KK. Skin substitutes: a brief review of types and clinical applications. Oman Med J **24,** 4, 2009.
9. Bello, Y.M., Falabella, A.F., and Eaglstein, W.H. Tissue-engineered skin current status in wound healing. Am J Clin Dermatol **2,** 305, 2001.
10. Reiffel, A.J., Henderson, P.W., Krijgh, D.D., Belkin, D.A., Zheng, Y., Bonassar, L.J., Stroock, A.D., and Spector, J.A. Mathematical modeling and frequenct gradient analysis of cellular and vascular invasion into integra and strattice: toward optimal design of tissue regeneration scaffolds. Plast Reconstr Surg **129,** 89, 2012.
11. Black, A.F., Berthod, F., L'Heureux, N., Germain, L., and Auger, F.A. *In vitro* reconstruction of a human capillary-like network in a tissue-engineered skin equivalent. FASEB J **12,** 1332, 1998.
12. Guillemette, M.D., Gauvin, R. Perron, C., Labbe, R., Germain, L., and Auger, F.A. Tissue-engineered vascular adventia with vaso vasorum improves graft integration and vascularization through inosculation. Tissue Eng Part A **16,** 2617, 2010.
13. Manasseri, B., Cuccia, G., Moimes, S., D'Alcontres, F.S., Polito, F., Bitto, A., Altavilla, D., Squadrito, F., Geuna, S., Pattarini, L., Zentillin, L., Collesi, C., Puliggada, U., Giacca, M., and Colonna, M.R. Microsurgical arterovenous loops and biological templates: a novel *in vivo* chamber for tissue engineering. Microsurgery 27, 623, 2007.
14. Leung, B.M., and Sefton, M.V. A modular engineering construct containing smooth muscle cells and endothelial cells. Ann Biomed Eng **35,** 2039, 2007.
15. Zheng, Y., Chen, J., Craven, M., Choi, N.W., Totorica, S., Diaz-Santana, A., Kermani, P., Hempsted, B., Fischbach-Teschi, C., Lopez, J.A., and Stroock, A.D. *In vitro* microvessesls for the study of angiogenesis and thrombosis. Proc Natl Acad Sci U S A **109,** 9342, 2012.
16. Sacharidou, A., Stratman, A.N., and Davis, G.E. Molecular mechanisms controlling vascular lumen formation in three-dimensional extracellular matrices. Cells Tissues Organs **195,** 122, 2012.
17. McGuigan, A.P., and Sefton, M.V. The thrombogenicity of human umbilical vein endothelial cell seeded collagen modules. Biomaterials **29,** 2453, 2008.
18. Cross, V.L., Zheng, Y., Choi, N.W., Verbridge, S.S., Sutermaster, B.A., Bonassar, L.J., Fischbach, C., and Stroock, A.D. Dense type I collagen matrices that support the cellular remodeling and microfabrication for studies of tumor angiogenesis and vasculogenesis *in vitro*. Biomaterials **31,** 8596, 2010.
19. Bellan, L.M., Singh, S.P., Henderson, P.W., Porri, T.J., Craighead, H.G., and Spector, J.A. Fabrication of an artificial 3-dimensional vascular network using sacrificial sugar structures. Soft Matter **5,** 1354, 2009.
20. Miller, J.S., Stevens, K.R., Yang, M.T., Baker, B.M., Nguyen, D.H., Cohen, D.M., E Torro, Chen, A.A., Galie, P.A., Yu, X., Chaturvedi, R., Bhatia, S.N., and Chen, C.S. Rapid casting of patterned vascular networks for perfusable engineered three-dimensional tissues. Nat Mater **11,** 768, 2012.
21. Bellan, L.M., Pearsall, M., Cropek, D.M., and Langer, R. A 3D interconnected microchannel network formed in gelatin by sacrificial shellac microfibers. Adv Mater **24,** 5187, 2012.
22. Takei, T., Sakai, S., Yokonuma, T., Ijima, H., and Kawakami, K. Fabrication of artificial endothelialized tubes with predetermined three-dimensional configuration from flexible cell-enclosing alginate fibers. Biotechnol Prog **23,** 182, 2007.
23. Luscher, T.F., and Vanhoutte, P.M. Endothelium-dependent contractions to acetylcholine in the aorta of the spontaneously hypertensive rat. Hypertension **8,** 344, 1986.
24. Bunag, R.D., and Butterfield, J. Tail-cuff blood pressure measurement without external preheating in awake rats. Hypertension **4,** 898, 1982.
25. Kabanov, A.V., Lemieux, P., Vinogradov, S., and Alakhov, V. Pluronic block copolymers: novel functional molecules for gene therapy. Adv Drug Deliv **54,** 223, 2002.
26. Cines, D.B., Pollak, E.S., Buck, C.A., Loscalzo, J., Zimmerman, G.A., McEver, R.P., Pober, J.S., Wick, T.M., Konkle, B.A., Swartz, B.S., Baranthan, E.S., McCrae, K.R., Hug, B.A., Schmidt, A.M., and Stern, D.M. Endothelial cells in the physiology and in the pathophysiology of vascular disorders. Blood **91,** 3527, 1998.
27. Ando, J., and Yamamoto, K. Vascular mechanobiology: endothelial cell responses to fluid shear stress. Circ J **73,** 1983, 2009.

28. Unger, R.E., Krump-Konvalinkova, V., Peters, K., and Kirkpatrick, C.J. *In vitro* expression of endothelial phenotype: comparative study of primary isolated cells and cell lines, including novel cell line HPMEC-ST1.6R. Microvasc Res **64,** 384, 2002.
29. Shepard, B.R., Jay, S.M., Saltzman, W.M., Tellides, G., and Pober, J.S. Human aortic smooth muscle cells promote arteriole formation by coengrafted endothelial cells. Tissue Eng Part A **15,** 165, 2009.
30. Institute of Laboratory Animal Research Committee for the Update of the Guide for Care and Use of Laboratory Animals. Guide for the Care and Use of Laboratory Animals. Eighth Edition, Washington, DC: The National Academies Press, 2011.

Address correspondence to:
Jason A. Spector, MD
Laboratory for Bioregenerative Medicine and Surgery
Division of Plastic Surgery
Weill Cornell Medical College
Payson 709-A, 525 E 68th Street
New York, NY 10065

E-mail: jas2037@med.cornell.edu

Received: September 16, 2013
Accepted: April 2, 2014
Online Publication Date: May 13, 2014